R. A. Schowengerdt*
Office of Arid Lands Studies and
Systems and Industrial Engineering Department
University of Arizona
Tucson, AZ 85719

Reconstruction of Multispatial, Multispectral Image Data Using Spatial Frequency Content

Multispatial, multispectral imagery is reconstructed by computer processing to enhance information extraction.

Abstract: *A data compression technique that utilizes a mixture of spatial resolutions (multispatial) for a multispectral scanner is described. The complementary reconstruction procedure that extrapolates edge information from the high resolution band(s) to the low resolution bands is also discussed. Examples of Landsat* MSS *imagery that have been compressed and reconstructed to the original resolution are presented. Error rates are calculated for two types of scenes, one containing prominent topographic effects, the other of an agricultural area. Improvement in radiometric quality of up to 40 percent is achieved by application of the reconstruction procedure to the compressed data.*

Introduction

There has been considerable interest in techniques for reducing the quantity of image data transmitted from spacecraft to ground receiving stations. The concern about excessive data acquisition/transmission rates is particularly important for the next generation of high spatial and radiometric resolution sensors, such as the thematic mapper (TM) on Landsat D, the multispectral resource sampler (MRS), SPOT (Chevrel, 1979), and Mapsat (Colvocoresses, 1979).

Techniques that reduce data quantity must also preserve image radiometry, resolution, and geometry within acceptable limits. A two-stage process is therefore indicated, the first stage being data compression and the second being data reconstruction. A large amount of research has been done on this general problem (Pratt, 1976; Pratt, 1978) and on satellite imagery in particular (Gonzalez and Wintz, 1977). Much of this work has described complex transform techniques that have found little operational application, but there is recent interest and success with simpler approaches (Hung, 1979).

It has been suggested (Colvocoresses, 1977) that a mixture of high spatial resolution spectral bands and lower resolution bands may be an acceptable way to reduce data rates without sacrificing image information content. The basis for this suggestion is that only one or two spectral bands are required to define the majority of edges in a scene, and hence only these bands need to be of high resolution. A significant advantage of mixed resolution, or what may be termed multispatial, compression is that it can be accomplished by appropriate specification of the sensor's instantaneous-field-of-view. (IFOV) and hence requires no on-board data processing. Multispatial sensors are already fairly common, examples being the combination of return beam vidicon (RBV)/multispectral scanner (MSS) on Landsat 3 and the thematic mapper (TM)/MSS planned for Landsat D (Table 1). The variable resolutions of these systems result, however, not from data compression considerations, but rather from the detector signal-to-noise ratio characteristics and manufacturing constraints.

This paper describes a relatively simple reconstruction technique for multispatial imagery. The

* This work was performed, in part, as an employee of the U.S. Geological Survey, Reston, Virginia.

Photogrammetric Engineering and Remote Sensing,
Vol. 46, No. 10, October 1980, pp. 1325-1334.

TABLE 1. RESOLUTIONS OF SOME CURRENT AND FUTURE SATELLITE SENSORS

Satellite	Sensor	Spectral bands	Instantaneous field-of-view IFOV (m)
Landsat 3	MSS	visible, near IR	80
		thermal IR	240
	RBV	visible	25
Landsat D	TM	visible, near IR	30
		thermal IR	120
	MSS	visible, near IR/ thermal IR	80/240
SPOT	Linear array	visible, near IR	20
		panchromatic	10
Mapsat (proposed)	Linear array	blue-green	30–90
		red	10–30
		near IR	30–90

technique utilizes computer processing to partially restore edge sharpness lost in the low-resolution imagery. It is applicable not only to the quantitative reconstruction of compressed data, but also to the enhancement of color composites of multispatial imagery. Digital composites of Landsat 3 RBV and MSS imagery are one current example of this application (Gehring and Perry, 1979).

RATIONALE

Edges in many natural scenes are caused by topography, e.g., shadows. Since these boundaries occur in all bands of a multispectral image, it is reasonable to assume that the high spatial frequency components (those contributing to edge sharpness) of such images are consistently correlated between spectral bands. The lower frequency components will carry much of the spectral (color) information and hence will show a greater variability of correlation between spectral bands. This situation is verified by analysis of a portion of a Landsat scene of the Grand Canyon (Figure 1a). A low-pass image, created by spatial filtering of the original with a 3-by-3 pixel averaging filter (Figure 1b), and a high-pass image, obtained by subtracting the low-pass image from the original (Figure 1c), were calculated for each spectral band. The two-dimensional histogram between low and high-pass images of several spectral bands was calculated, examples of which are shown in Figure 2. A linear regression was then applied to the histograms to determine the degree of fit to a straight line. The results (Figure 3) support the supposition that, for scenes with topographic relief, edges correlate more consistently from band to band than does low frequency information. Note that for uncorrelated bands, edges possess a greater degree of correlation than do low frequencies, and for correlated bands the opposite is true.

The same arguments for an area of flat topography that contains human activities, such as agriculture or urbanization, are not necessarily valid. However, it is apparent that many edges, such as those between agricultural fields or roads and surrounding vegetation or soil, will exist, at varying contrast, in all the spectral bands. The problem here is that these edges are color edges and the information that defines them changes from band to band. For example, the contrast of the edge may completely reverse polarity as seen in the Landsat image of agriculture in Figure 4. An approach is developed later to deal with this more complex situation.

PROCEDURE

A simulation of multispatial, multispectral imagery was made with the Landsat images of Figures 1 and 4. Reconstruction of the low resolution data was then performed with the techniques described below.

SIMULATION OF COMPRESSED, MULTISPATIAL IMAGERY

Band 5 (red) was retained at its original resolution of 80-by-80 m and bands 4, 6, and 7 were reduced to 240-by-240 m resolution by a 3-by-3 pixel low-pass filter (Figure 1b). These data were then resampled at 240 m to represent the data as acquired by a mixed resolution sensor. The quantity of data in bands 4, 6, and 7 is, therefore, reduced to one-ninth that of the original imagery. This step of the process is depicted in Figure 5. The bottom image in Figure 5 represents the data transmitted to the ground for bands 4, 6, and 7, along with the high resolution band 5 (similar to the upper image of Figure 5). Experience has shown that band 5 generally has more scene contrast than the other bands, making it the logical choice for the high resolution band.

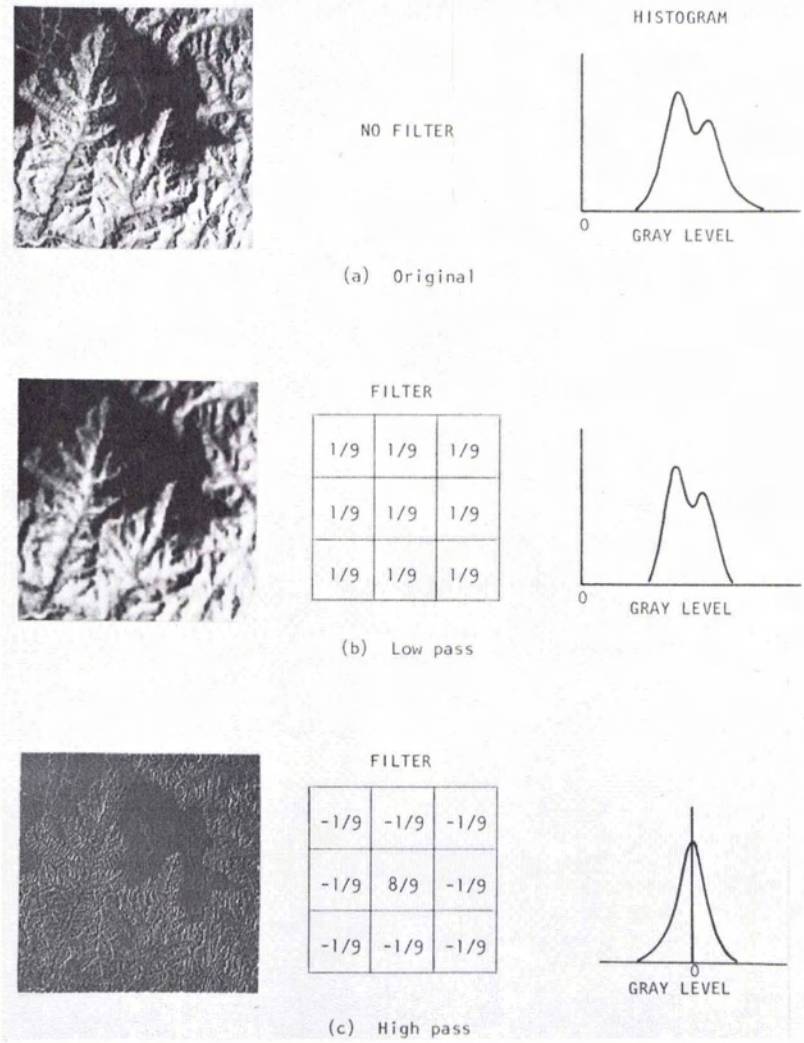

FIG. 1. Examples of low and high pass images and their gray level histograms.

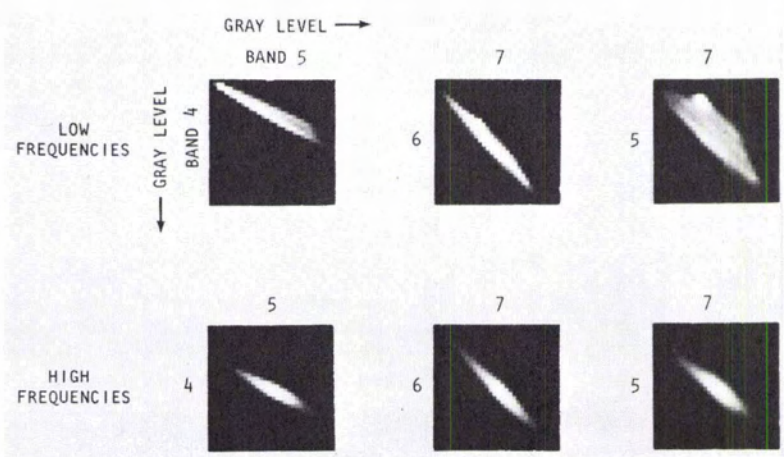

FIG. 2. Correlation histograms between bands for low and high frequency components (Landsat ID #2478-17205).

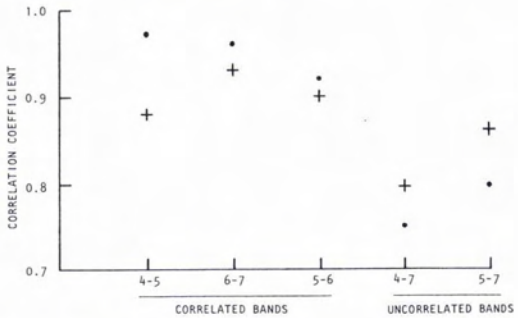

FIG. 3. Degree of correlation between bands for low (·) and high (+) frequency components (Landsat ID #2478-17205).

Although the resolutions simulated with these Landsat data are a factor of three or four lower than anticipated with the TM or MRS, the comparative results obtained in this study should remain valid at higher resolutions.

RECONSTRUCTION OF COMPRESSED IMAGES

This section describes ground-based computer processing to restore the resolution lost in the compressed data. The first step is to resample the imagery at the higher sampling rate of band 5. This is accomplished by some type of interpolation, such as nearest-neighbor, bilinear, or cubic spline (Bernstein, 1976). Examples of each are shown in Figure 6. Nearest-neighbor interpolation amounts in this case to replication of pixels and lines, and the image exhibits characteristic blockiness. Bilinear and cubic spline interpolation yield more realistic images, with cubic spline interpolation

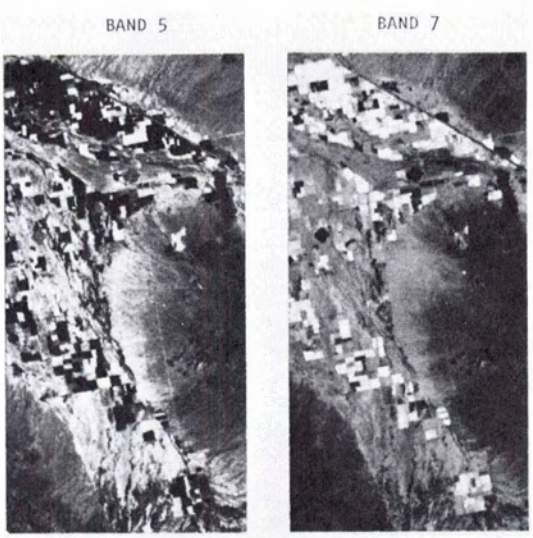

FIG. 4. Band 5 and 7 data (Landsat ID #1030-17271) illustrating contrast reversal at vegetation/soil boundaries.

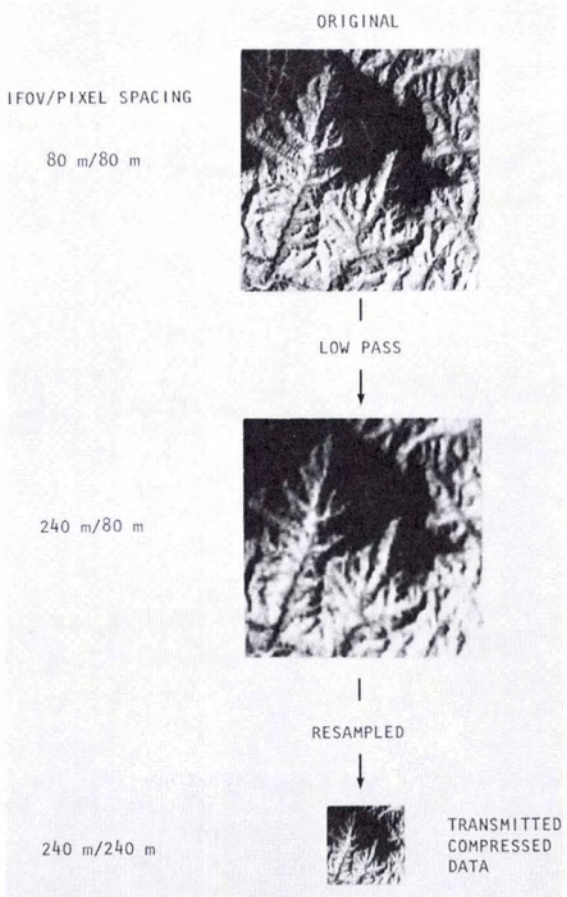

FIG. 5. Simulation of compressed data from Landsat image.

producing a slightly sharper enlargement. Several types of interpolation have been compared for geometric correction of Landsat data (Simon, 1975; Shlien, 1979) and cubic spline has been shown to be a good compromise between error rate and computational cost. It is also the technique used at the EROS Data Center for production of enhanced Landsat products (Holkenbrink, 1978).

At this point, it is instructive to note that the goal of the interpolation process is to reproduce as closely as possible a low-pass filtered image (Figure 1b), as if the data have not been resampled to achieve compression. This is clear from the type of edge restoration described below. The three types of interpolation are compared for the Grand Canyon image in terms of this criterion in Table 2. Bilinear interpolation is an improvement over nearest-neighbor by about 10 percent, while cubic spline results in only a small additional improvement. The disappointing performance of the cubic spline algorithm in this case can be explained by the fact that virtually all spatial frequency content in the image corresponding to structure less than three pixels wide has been lost in the compression

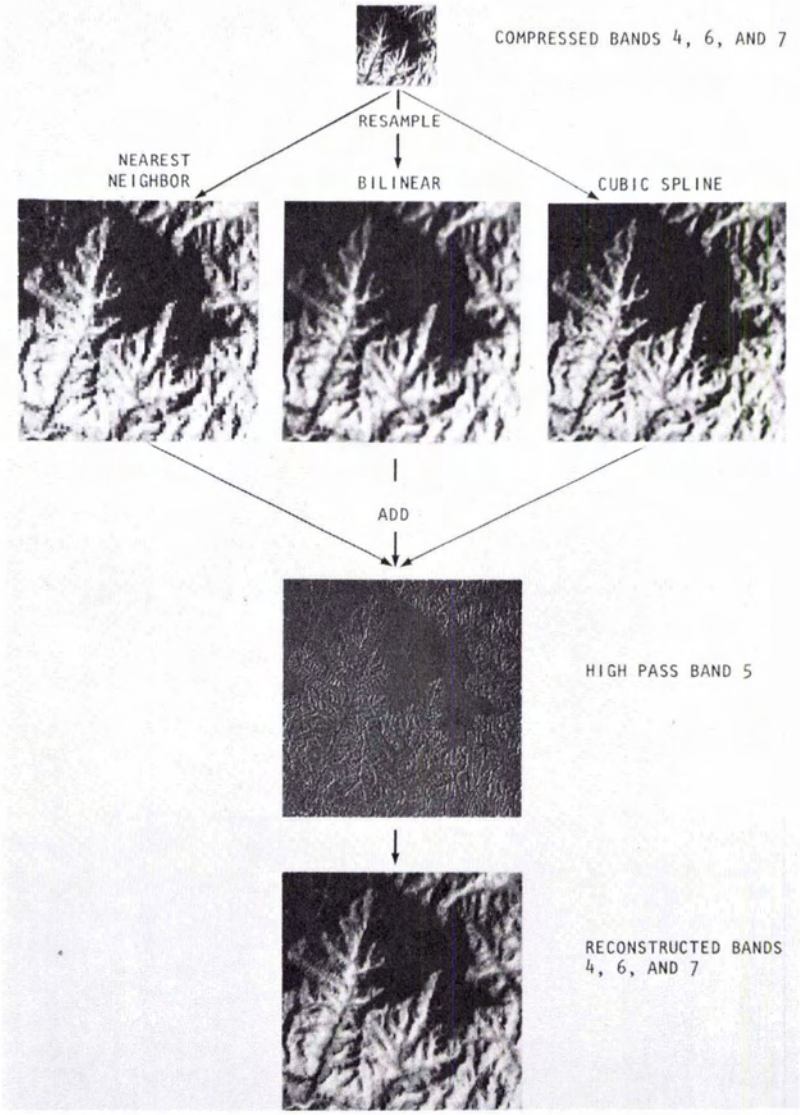

FIG. 6. Reconstruction of compressed data.

process. There is, thus, little edge structure remaining, and edge structure preservation is the chief advantage of cubic spline interpolation. Bilinear interpolation is used in all the remaining examples of the study because of the negligible advantage of cubic spline in this application and its greater computational cost (about four times over bilinear).

TABLE 2. RMS ERRORS BETWEEN LOW-PASS IMAGES AND RESAMPLED COMPRESSED IMAGES (LANDSAT ID # 2478-17205) (MSS GRAY LEVEL UNITS, 0-127)

	Resample algorithm		
Band	Nearest neighbor	Bilinear	Cubic spline
4	2.19	1.96	1.93
5	4.00	3.58	3.52
6	4.66	4.17	4.10
7	4.44	3.97	3.90

The final step in the reconstruction process is restoration of the high frequency components in the resampled compressed data (Figure 6). Based on the high frequency component correlations of Figures 2 and 3, a high-pass image of band 5 may be used to approximate the edges lost in the compressed data. This procedure represents an extension of a technique previously applied to monochromatic imagery (Graham, 1967) to multispectral imagery. Note that a given image, i, may be considered a sum of two components (Hunt and Cannon, 1976)

$$i = \text{low-pass } (i) + \text{high-pass } (i).$$

This is obviously true for the filters of Figure 1. In the present study, the high-pass component of a given compressed spectral band is approximated by the high-pass version of band 5. It can now be seen why the resampled compressed images of Figure 6 should be as similar as possible to low-pass images.

To extrapolate the high frequency components of band 5 to the other bands, the amplitudes must be scaled to account for the differences in contrast between bands. Table 3 lists the variances of the low and high-pass images of each of the original bands (no compression) for the image of Figure 1. Also listed is the variance for the corresponding resampled compressed image, which very nearly equals that of the low-pass image. Since the high-pass data histogram invariably exhibits a Gaussian shape with zero mean (Hunt and Cannon, 1976; Figure 1c), the amount of edge amplitude added to each band, j, can be controlled by a multiplicative constant, K_j, i.e.,

$$i_j \simeq \text{low-pass } (i_j) + K_j \times \text{high-pass } (i_5)$$

where j indicates band 4, 6, or 7. A reasonable assumption would be that the value of K_j should be equal to the ratio of the standard deviations, σ_j (high-pass)/σ_5 (high-pass), but the standard deviation σ_j (high-pass) is not available since band j is compressed. An alternative is, then,

$$K_j = \sigma_j/\sigma_5 \text{ (high-pass)} \simeq \sigma_j/\sigma_5 \text{ (low-pass)},$$

which makes use of the available data and the idea that contrast should equally affect low and high frequency components. Table 3 indicates that this relationship is not exactly verified experimentally, particularly for less correlated bands. A search for a more satisfactory alternative is planned for future studies.

Results

The resulting images from the compression/reconstruction process as described above are shown in Figures 7 and 8 for bands 4 and 7 of the two scenes studied. The visual improvement achieved by extrapolating edge information from the high resolution band 5 to the compressed bands is obvious and substantiated by generally reduced RMS errors (Table 4). A false color composite of bands 4, 5, and 7 (displayed as blue, green, and red, respectively), before and after reconstruction, is shown in Plate 1 for a threefold and fivefold resolution reduction in bands 4 and 7. The original Landsat data are included for comparison with the reconstructed data.

A fringing effect is evident in the reconstructed band 7 images (Figures 7 and 8), particularly for the agricultural scene, an enlarged portion of which is shown in Figure 9a. This artifact is due to the color nature of the edges as described previously and may be explained with the aid of Figure 10. Because the edges between vegetated fields and soil reverse contrast between bands 5 and 7, the high frequency components from band 5 that are added back to band 7 are of the opposite sign to the correct components. An adaptive procedure was developed to detect such boundaries and change the sign of the high frequency component accordingly. The high-pass versions of the *resampled compressed* band 7 image and the *low-pass* filtered band 5 image are calculated. The sign of each pixel in these high-pass images then represents the direction of the local low frequency gradient (Figure 10b). Note from Figure 10 that, if the two high-pass images are multiplied together, the result will always be positive for gradients in the same direction and negative for gradients in opposite directions. This is, therefore, a mechanism for detecting contrast reversal at boundaries.

The binary version of the high-pass product image is shown in Figure 9c. Bright pixel values ($K = +1$) represent areas of similar gradient in bands 5 and 7 and black areas ($K = -1$) indicated areas where the contrast reverses. To remove the scattered noise in Figure 9c, all pixels with a magnitude greater than -0.25 were set to $+1$, resulting in Figure 9d. Figure 9d thus represents a mask of K values to weight the high-pass components of band 5 when they are added to band 7. The result is Figure 9b where it is seen that much of the fringing at field boundaries has been eliminated.

This procedure was applied to the band 7 reconstruction for both Landsat scenes with the results shown in Figure 11 and the associated accuracies given in the last column of Table 4. Note that the adaptive modification of K results in a lower RMS error only for the most severely uncorrelated im-

Table 3. Image Component Variances (Landsat ID # 2478-17205) (MSS Gray Level Units, 0-127)

Band	Variance			Standard deviation ratio band j/band 5	
	Low pass	Resampled compressed	High pass	Low pass	High pass
4	59.6	59.7	7.5	0.54	0.57
5	204.1	204.4	23.1	1.00	1.00
6	161.3	161.4	32.9	0.89	1.19
7	125.6	125.7	30.4	0.78	1.15

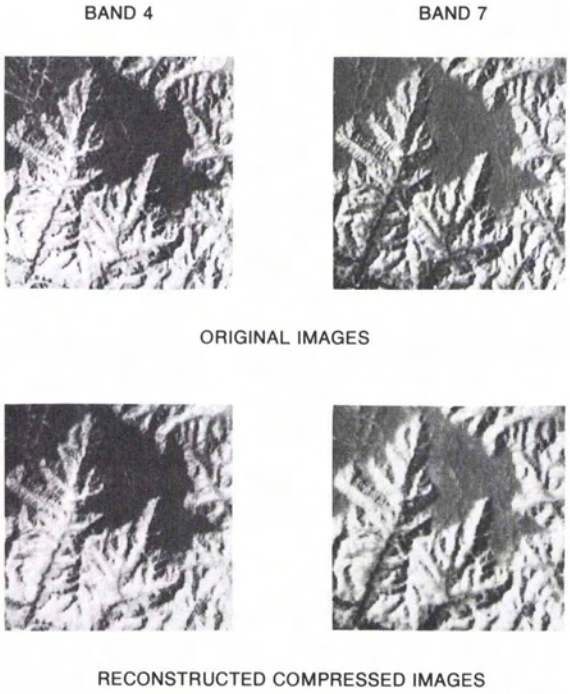

FIG. 7. Original and reconstructed compressed images (Landsat ID #2478-17205).

ages, bands 5 and 7 of the agricultural scene. It should be kept in mind that the RMS error is calculated over the entire area shown in the figures and, hence, represents an average over these areas. The improvement in RMS error for band 7 resulting from adaptively modifying K is greater in the vicinity of color edges than for the area as a whole.

SUMMARY

A procedure is described for edge reconstruction in a mixed resolution set of multispectral images. Essentially, edge information contained in a high resolution band is extrapolated to the low resolution bands. A refinement is also outlined for

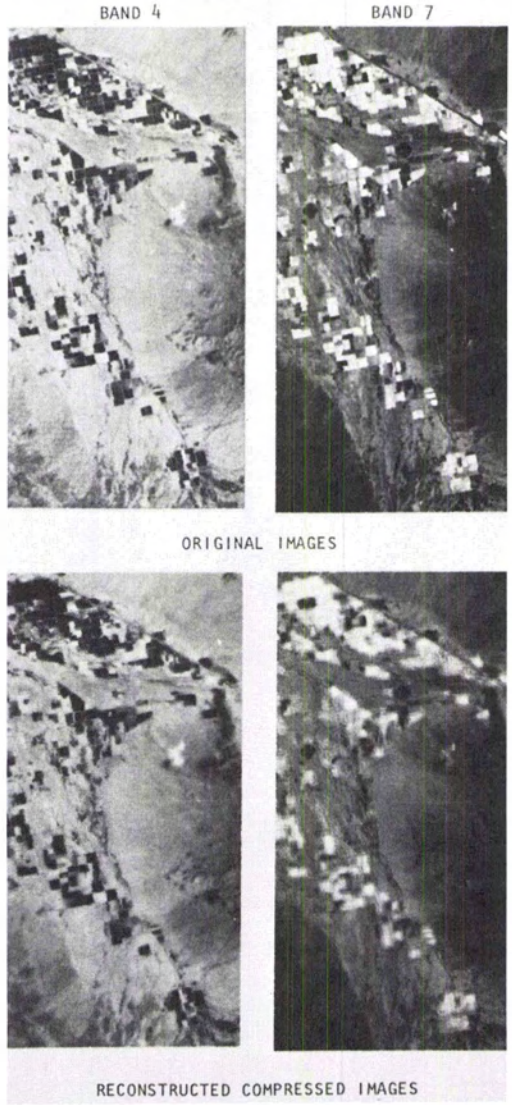

FIG. 8. Original and reconstructed compressed images for Avra Valley (Landsat ID #1030-17271).

TABLE 4. RMS ERRORS BETWEEN ORIGINAL, RESAMPLED COMPRESSED, AND RECONSTRUCTED IMAGES (MSS GRAY LEVEL UNITS, 0-127)

		Rms error between original and		
Landsat ID #	Band	Resampled compressed	Reconstructed (nonadaptive)	Reconstructed (adaptive)
2478-17205	4	3.83	2.37	2.95
	6	8.11	5.35	6.63
	7	7.76	5.43	6.47
1030-17271	4	3.76	2.44	3.00
	6	5.97	5.99	6.14
	7	4.39	5.31	4.88

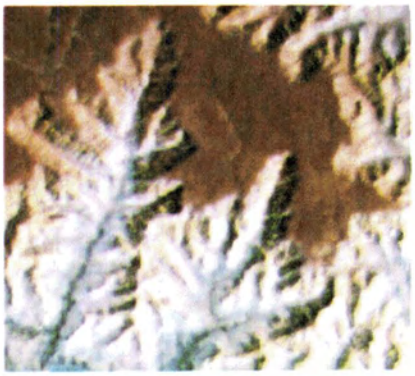

Bands 4,7 - 240m resolution
Band 5 - 80m resolution

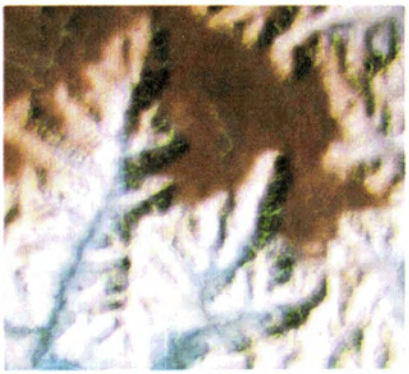

Bands 4,7 - 400m resolution
Band 5 - 80m resolution

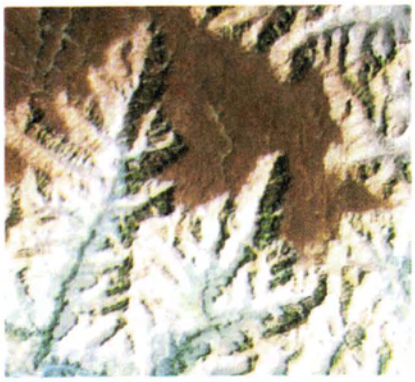

Bands 4,7 reconstructed
Band 5 - 80m resolution

Bands 4,7 reconstructed
Band 5 - 80m resolution

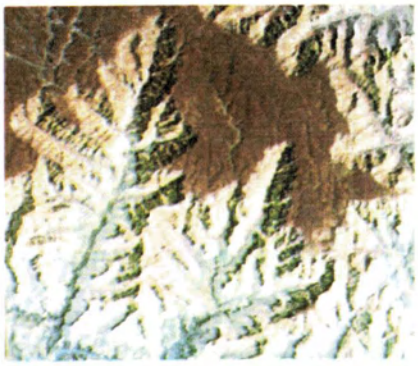

Bands 4,5,7 - 80m resolution
Original Data

PLATE 1. Color composites of bands 4, 5, and 7 with and without reconstruction (4-blue, 5-green, 7-red).

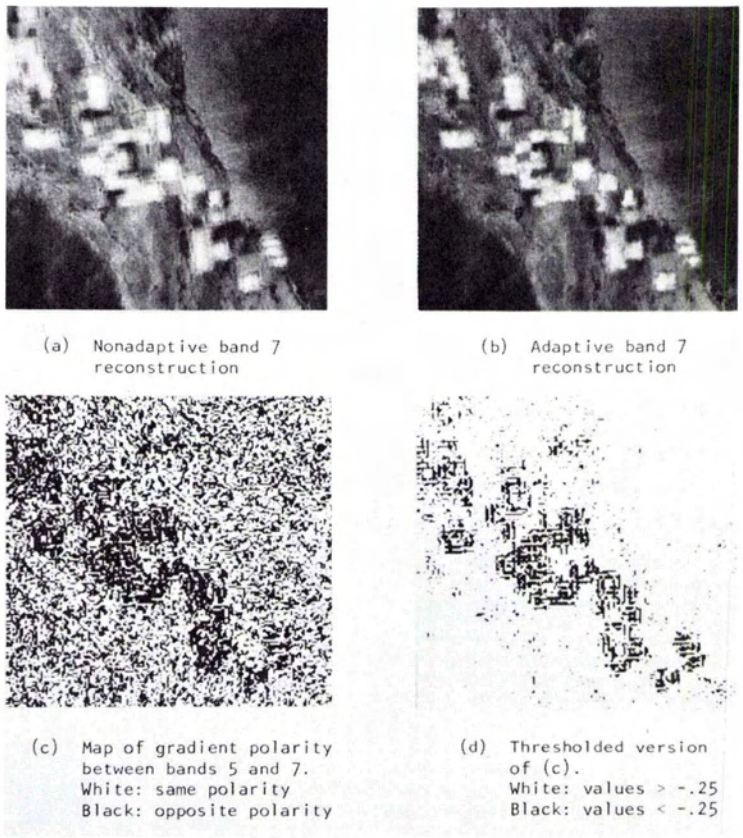

FIG. 9. Adaptive reconstruction procedure.

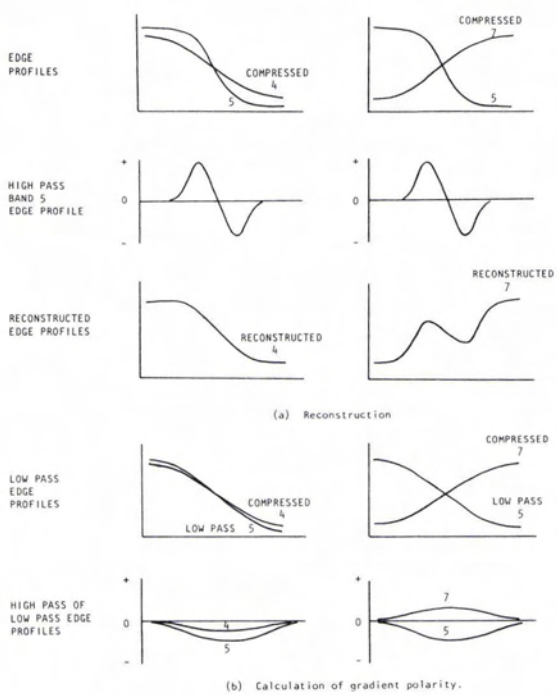

FIG. 10. Analysis of band-to-band contrast polarity.

dealing with contrast reversal at vegetation/soil boundaries between visible and near infrared images. These procedures are applied in a multispatial, multispectral simulation using two Landsat

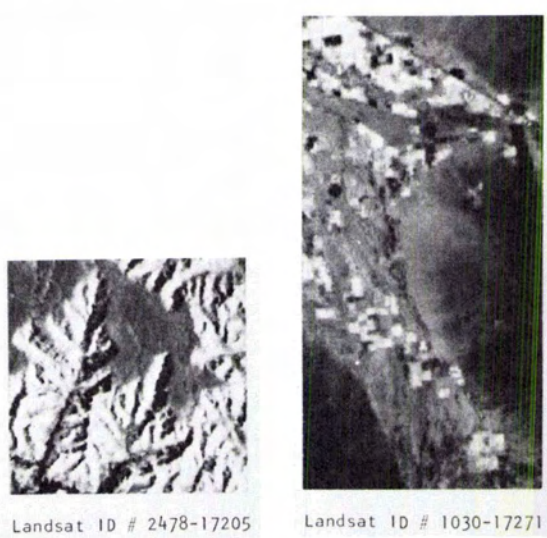

FIG. 11. Adaptive band 7 reconstructions.

MSS images, one of which is dominated by topographic shading, and the other by color information, with little topographic relief. These test data were selected as representative of the range of relevant scene types for a multispatial, multispectral analysis, and, although a limited set of data, permit the following conclusions to be made:

(1) A great deal of high frequency information can be obtained with only one high resolution band, and this information can be extrapolated to low resolution bands, with a considerable improvement in visual and radiometric quality.

(2) Edges which reverse contrast between bands, notably vegetation/soil boundaries, are difficult to reconstruct with a single high resolution band. Either relatively complex computer processing or a sensor with a high resolution band in each region of the spectrum (e.g., visible and near IR) is necessary.

(3) Multispatial sensor design can yield a data compression rate of about 3:1 for a four band image with one high resolution band, and requires no complex computer processing on board the satellite.

Although the present simulation was performed with Landsat MSS data, the techniques described are applicable to enhanced combinations of images from dissimilar sensors, such as from the MSS, RBV, Seasat or aerial radar systems, Thematic Mapper, or SPOT. The primary requirement is that a strong correlation of edge structure exists between spectral bands, and that the imagery to be combined are accurately registered. Additional studies are underway to determine the limitations and potential of the multispatial concept for a wide range of scene types and dissimilar spectral bands.

ACKNOWLEDGMENTS

This research was originally suggested by A. P. Colvocoresses and was supported in part by the U.S. Geological Survey, Reston, Virginia. The color images of Plate 1 were made in the Digital Image Analysis Laboratory of the University of Arizona. The author is grateful to A. P. Colvocoresses of the U.S. Geological Survey and to P. N. Slater of the University of Arizona for valuable comments on this manuscript.

REFERENCES

Bernstein, R., 1976. Digital image processing of earth observation sensor data. *IBM J. Res. Devel.* 20:74-89.

Chevrel, M., 1979. A presentation of the French satellite for earth observation: the SPOT program. *Proceedings of the Annual Meeting*, American Society of Photogrammetry.

Colvocoresses, A. P., 1977. Proposed parameters for an operational Landsat. *Photogramm. Eng. Remote Sensing* 43:1139-1145.

———, 1979. Proposed parameters for Mapsat. *Photogramm. Eng. Remote Sensing* 45:501-506.

Gehring, Dale, and Lincoln Perry, 1979. EROS Data Center, private communication.

Gonzalez, R. C., and P. Wintz, 1977. *Digital Image Processing*, Addison-Wesley, Reading, Massachusetts, 431 p.

Graham, D. N., 1967. Image transmission by two-dimensional contour coding. *Proc. IEEE* 55:336-346.

Holkenbrink, Patrick F., 1978. *Manual on Characteristics of Landsat CCTs Produced by the EROS Data Center Digital Image Processing System.* U.S. Geological Survey, Revised December 1978, 70 p.

Hung, Stephen H. Y., 1979. A generalization of DPCM for digital image compression. *IEEE Trans. Pattern Anal. Machine Intelligence* PAMI-1:100-109.

Hunt, B. R., and T. M. Cannon, 1976. Nonstationary assumptions for Gaussian models of images. *IEEE Trans. Syst. Man Cybern.* SMC-6:876-882.

Pratt, William K., 1976. Survey and analysis of image coding techniques. *Proc. SPIE* 74:178-184.

———, 1978. *Digital Image Processing*, Wiley-Interscience, New York, 750 p.

Shlien, Seymour, 1979. Geometric correction, registration, and resampling of Landsat imagery. *Canadian J. Remote Sensing* 5:74-89.

Simon, K. W., 1975. Digital image reconstruction and resampling for geometric manipulation. *Proc. 1975 Machine Processing of Remotely Sensed Data Symposium*, IEEE 75CH 1009-O-C, 3A-1-11.

(Received 5 December 1979; revised and accepted 14 April 1980)

Publication Available

An Annotated Bibliography of Remote Sensing for Highway Planning and Natural Resources, by Daniel L. Civco, William C. Kennard, and Michael Wm. Lefor, has just been published as Storrs Agricultural Experiment station Bulletin No. 456. The Bibliography is a collection of 152 abstracts organized into the following subject areas:

- Highways and remote sensing applications
- Environmental impact of highways and corridor selection methods
- Wetlands and remote sensing applications
- Economics of remote sensing
- General remote sensing applications

and includes an Author Index, Keyword Index, and List of Abbreviations and Acronyms.

The Bibliography is available for $4.00 from

Agricultural Publications Department, U-35
College of Agriculture and Natural Resources
The University of Connecticut